

**A novel copper(II)-Schiff base complex containing pyrrole ring: Synthesis,  
characterization and its modified electrodes applied in oxidation of aliphatic alcohols**

**Ali OURARI<sup>a</sup>, Djouhra AGGOUN<sup>a,\*</sup>, Lahcène OUAHAB<sup>b</sup>**

*<sup>a</sup>Laboratoire d'Electrochimie, d'Ingénierie Moléculaire et de Catalyse Redox (LEIMCR),  
Faculté de Technologie, Université Ferhat Abbas Sétif-1, Route de Béjaia Sétif 19000-  
Algérie.*

*<sup>b</sup>Institut des Sciences Chimiques de Rennes, UMR 6226 CNRS, Université de Rennes-1, 263  
Avenue du Général Leclerc 35042 Rennes Cedex, France.*

**Abstract**

A new copper(II) complex Cu(II)-L containing N<sub>2</sub>O<sub>2</sub> donor atoms has been prepared from 6-[3'-(N-pyrrol)propoxy]-2-hydroxyacetophenone and diaminoethane in the presence of copper acetate monohydrate. It was characterized by spectroscopic methods such as FT-IR, UV-vis, mass spectra, elemental analysis and cyclic voltammetry. The molecular structure of Cu(II)-L has also been confirmed by X-ray diffraction analysis. The electrochemical behavior of copper(II)-Schiff base complex containing pyrrol groups has been investigated in DMF and acetonitrile solutions using cyclic voltammetry. Thus, conducting polymeric films of polypyrrole were obtained on the surfaces of glassy carbon and ITO electrodes using copper(II)-complex as monomer. The modified electrodes were electrochemically and morphologically characterized and their electrocatalytic properties in heterogeneous phase have also been investigated. The AFM studies show that the morphology of polypyrrole (PPy) films on ITO-electrodes depends on the number of cyclical scans. The electrocatalytic performances of this complex seem to be more efficient towards the electro-oxidation of isopropyl alcohol than any other kinds of alcohols such as methanol, ethanol and benzyl alcohol. The electro-reduction of carbon dioxide was also examined.

**Keywords:** Copper(II)-Schiff base complex, Pyrrolic monomers, Modified electrodes, X-ray diffraction, Oxidation of aliphatic alcohols.

---

Corresponding author. Tel: +213.067.78.81.45.

E-mail address: [aggoun81@yahoo.fr](mailto:aggoun81@yahoo.fr) (D. Aggoun).

During the last years, Schiff base ligands were found to be an important class of chelating agents in coordination chemistry [1,2]. These compounds have also played a considerable role in the development of chemistry. Thus, a large number of these Schiff base ligands and their complexes have been studied in the past because of their wide application owing to their interesting properties as in electrocatalysis [3], inhibitors of corrosion [4], and biosensors [5]. So, a particular interest was paid to the complexes obtained from tetradentate ligands (OONN) containing oxygen and nitrogen as heteroatom donors. However, these complexes have extensively been used as catalysts for a wide variety of reactions, including olefins epoxidation [6], polymerization [7], oxygen activation [8] and carbon dioxide [9].

So, in continuation of our recent papers [10], we have undertaken a covalent grafting of electropolymerizable units as pyrrole, aniline and thiophene on Schiff base ligands in order to elaborate their modified electrodes for applications essentially focused on the heterogeneous catalysis and electrocatalysis. In this context, the transition metal complexes anchored on the polymer matrices constitute an active area of research due to their structural, magnetic properties and potential catalytic models of several biological systems as, for example, cytochrome P450 reactions [11]. The oxidative electropolymerization of various metal–salen complexes has been investigated [12] and the electrochemical design of modified electrodes by electrodeposition of polymer films has also been widely developed while those of conducting polymers are little studied. For this reason, this work aims to elaborate new materials as coordination compounds bearing pyrrol units which have been found to be very useful for catalytic applications in various fields of organic, inorganic and bioorganic synthesis [13].

Thus, a copper(II)-Schiff base complex (**1b**) was synthesized [14] by the reaction of 6-(3'-N-pyrrolpropoxy)-2-hydroxyacetophenone [15] and ethylenediamine using absolute ethanol as solvent. This mixture was refluxed for about 1 hour until completion of the reaction after

which, one mmol of copper acetate monohydrated ( $\text{Cu}(\text{OAc})_2 \cdot 1\text{H}_2\text{O}$ ) was added. After cooling, the copper complex was precipitated by diethyl oxide and the resulting solid was recovered by filtration, yielding 85 mg (61%).

### Scheme 1

The analytical data of the new copper(II)-Schiff base complex were in good agreement with the proposed molecular formula. This molecular structure was also confirmed by the X-ray diffraction analysis.

The FT-IR spectrum of the complex shows a strong absorption band at  $1602\text{ cm}^{-1}$ , it may be due to the coordination of the copper(II) ion by the azomethine ( $\text{C}=\text{N}$ ) nitrogen atom [16]. However, the absorption band appearing at  $1249\text{ cm}^{-1}$  was assigned to the C-N stretching; while, the strong band located at  $1096\text{ cm}^{-1}$  is assigned to the stretching mode of the phenoxy group. The formation of the M-O and M-N bonds were further supported by the appearance of the  $\nu$  (M-O) and  $\nu$  (M-N) bands at  $570$  and  $625\text{ cm}^{-1}$  respectively as reported in the literature [16].

The formation of the copper(II) complex was also confirmed by UV-vis analysis since their electronic spectra, recorded in DMF solution, show three absorption bands at 288, 351 and 550 nm. At short wavelengths, an intense absorption band is attributed to  $\pi-\pi^*$  transitions of the aromatic moieties, while a wide absorption band  $n-\pi^*$  arising from electronic transitions involving the conjugated system of the complex with azomethine groups. The transitions observed in the visible region around 550 nm were attributed to the weak d-d transitions and it expresses that the copper atom is well coordinated to the ligand ( $\text{H}_2\text{L}$ ). These results are in good agreement with the literature [17,18].

The FAB-mass spectrum of the complex Cu(II)-L shows a peak at  $m/z = 606.6$  (20.00%) corresponding to the weight of the molecular ion ( $\text{M}^+$ ). Another peak was also observed at  $m/z 1209.9$ (11.53%) suggesting the binuclear form  $[\text{Cu}(\text{II})\text{-L}]_2$ . Further fragmentations of this

copper complex generates a stronger peak  $m/z$  543.7(100%) corresponding to the base peak  $[L+H]^+$  ion. The mass spectrum of the Cu(II)-L shows again several peaks representing successive degradation of the complex molecule leading to the formation of different fragments such as  $m/z$  272.6(13.46%), 330.6 (17.30%), 344.4(9.23) and 367.6(3.07%).

Prismatic colourless single crystals of Cu(II)-L suitable for X-ray diffraction were obtained by slow evaporation from acetonitrile solution and crystallizes in the triclinic space group P-1 with 2 formula units in the cell [19]. The copper complex was characterized by X-ray diffraction, and the ORTEP representation with the atomic numbering is given in fig. 1. Relevant X-ray diffraction data are listed in Table 1. The crystal structure of Cu(II)-L shows a tetradentate OONN coordination of the Schiff base ligand. The coordination environment of Cu is satisfied by the phenoxo oxygen and imine nitrogen atoms of the Schiff base ligand [Cu: O1, O2, N1, N2]. The azomethine linkage is evident from the N1–C14 and N2–C18 bond lengths (1.303(5) and 1.309(5) Å, respectively), C17–N1–C18 and C14–N2–C16 angles (118.4(3) and 119.7(3)°, respectively). The bond lengths involving the phenyl carbon and phenoxo oxygen atoms, C12–O1, C8–O3, C21–O2 and C25–O4 are 1.309(5), 1.378(5), 1.317(5) and 1.372(5) Å, respectively and these values are in the range of the usually observed standard C(sp<sup>2</sup>)–OH and C(sp<sup>2</sup>)–O– bond length [20]. The Cu–O and Cu–N bond lengths for Cu(II)-L vary in the range 1.892(3)– 1.899(3) for C–O and 1.937(3)–1.947(3) for C–N, respectively. These values are also in good agreement with related reported complexes [21]. Cisoid and transoid angles for Cu deviate also from their ideal values of 90° and 180° and are found to be in the range 86.22(13)– 92.54(12)° and 168.64(13)–170.02(13)°, respectively. The bond lengths and angle around C17 are in agreement with sp<sup>3</sup> hybridizations of this atom. The molecule is not planar, the two phenyls rings (C8→C13 and C20→C25) and the two five members ring of the pyrrol (N3, C1→C4 and N4, C29→C32)

are almost orthogonal. Some overlap of one  $sp^3$  orbital of oxygen with  $\pi$ -system of phenyl ring may be considered.

### Figure 1

### Figure 2

The monomer Cu(II)-L was studied by cyclic voltammetry in acetonitrile solutions and at a scan rate of  $100 \text{ mVs}^{-1}$  exploring the potentials ranging from  $-1.800 \text{ V}$  to  $+1.600 \text{ V}$ . Hence, the voltammogram obtained, given in fig.3, shows five oxidation waves observed at  $E_{pa1} = -0.975$ ,  $E_{pa2} = -0.697$ ,  $E_{pa3} = +0.323$ ,  $E_{pa4} = +0.841$  and  $E_{pa5} = +1.525 \text{ V/SCE}$  respectively. The first is ascribed to the reoxidation of Cu(I)/Cu(0), the second to the reoxidation of Cu(II)/Cu(I) while the third one may be attributed to the oxidation of Cu(III)/Cu(II). These results may be approached to those reported in the literature [22]. As for the wave located at  $+0.841 \text{ V/SCE}$ , it corresponds to the anodic oxidation of pyrrole moieties leading to the formation of poly(pyrrole) films. The last one may be assigned to the oxidation of the Schiff base ligand. For the return sweep, only two reduction waves were observed at  $E_{pc1} = -0.904$  and  $E_{pc2} = -1.143 \text{ V/SCE}$ . The first is attributed to the reduction of Cu(II)/Cu(I) species and the second to the reduction of Cu(I) yielding Cu(0). Concerning oxidation wave of pyrrole, it seems to be an irreversible system [23].

### Figure 3

Cyclic voltammograms, recorded in the range between  $0.0$  and  $+1.0 \text{ V}$ , show a redox couple exhibiting two waves Cu(II)/Cu(III) at  $+0.48 \text{ V}$  and Cu(III)/Cu(II) at  $+0.36 \text{ V}$ . The peak-to-peak separation ( $\Delta E_p$ ) was found to be  $120 \text{ mV}$ . On the other hand, in spite of the  $\Delta E_p$  data being larger than the theoretical value for an electrochemically reversible one-electron process. Thus, for this complex the large  $\Delta E_p$  value expressing an electrochemical oxidation of Cu(II) would be due to a quasi-reversible behavior of the couple  $\text{Cu(III)L} + e^- = \text{Cu(II)L}$ . This fact implies that these electrochemical processes are mainly diffusion-controlled

[18]. In addition, in the range 0.0 to -1.5 V, it was observed that the copper(II) complex shows two irreversible reduction waves in the cathodic potentials region as reported in the literature for similar structures [24].

Fig.4 (Curve a) shows the evolution of the cyclic voltammograms of Cu(II)-L complex in acetonitrile solution. During the repeated potential scans between -0.1 and 1.1 V, the anodic oxidation shows an obvious decrease of the peak current expressing probably an electrocatalytic effect causing an overoxidation of the poly(pyrrole) matrices. In this case, on the Fig.4 (Curve a) the electropolymerization of Cu(II)-L was achieved by repetitive cycling of the potential at the surface of a glassy carbon electrode between +0.6 and -1.8 V at  $100 \text{ mVs}^{-1}$ . The buildup of the electropolymerized poly-[Cu(II)-L] films was confirmed by continuous increasing of the peak current and repeated cycling produces an electroactive polymer on the glassy carbon electrode surface. When the poly-[Cu(II)-L] films were electrodeposited on the surface of this electrode, it was copiously rinsed with bi-distilled water, acetonitrile and immediately transferred to another fresh electrolytic  $\text{CH}_3\text{CN}$  solution containing no monomer.

Similarly, poly-[Cu(II)-L] films are electrodeposited on optically transparent electrodes like those of indium tin oxide (ITO). The growing of the poly-[Cu(II)-L] films on ITO-electrode as  $\pi$ -conjugated conductor polymers have been carried out and evidenced by the continuous increasing of the peak currents ( $i_{pa}$ ,  $i_{pc}$ ) yielding poly-[Cu(II)-L] films. The ME (poly-Cu(II)-L/ITO) obtained was identified by an electrochemical technique using cyclic voltammetry indicating the presence of electrodeposited poly-[Cu(II)-L]. Thus, different polymer thicknesses can be obtained by controlling the number of the electropolymerizing scans. These experiments were performed in acetonitrile solutions  $10^{-1} \text{ M}$  TBAP using  $10^{-3} \text{ M}$  of copper complex Cu(II)-L.

**Figure 4**

Atomic force microscopy was used to explore the morphology of the poly-[Cu(II)-L] films electrodeposited onto ITO-substrate. The values of roughness and film thickness are summarized in Table 2.

### **Table 2**

### **Figure 5**

From the micrographs, it can be clearly observed that there is a significant increase in roughness and film thickness values as the number of voltammetric scans increases. A typical 3-D AFM micrograph is shown in the Fig.5. Where, it becomes clear that the nuclei are produced with different forms and sizes at the surface of the electrode.

The oxidations of methanol, ethanol, isopropanol and benzyl alcohol were performed using copper(II) complex as catalyst in an aqueous media. These electrochemical experiments have confirmed the presence of electrocatalytic behavior for the different alcohols indicated above as it can also be observed from Fig.6.

### **Figure 6**

The effect of the concentration of alcohol was studied with the four types of alcohols. Their electro-oxidation reactions were carried out using Cu(II)-L as catalytic sites which were uniformly dispersed on the surface of the modified electrode. For this purpose, volumes ranging from 10 $\mu$ L to 40 $\mu$ L were progressively added in order to evaluate the concentration effect as function of the efficiency of the electrooxidation reaction. Fig.6 (curves a, b, c and d) shows the plots of the anodic oxidation charge obtained for different concentrations of each alcohol. The efficiency of this reaction was estimated from the  $Q_{ox}$  values (integrated charge under the oxidation wave at low scan rate), recorded at each concentration applied for all alcohols studied. From these observations, it can be concluded that the anodic oxidation charge increases as the alcohol concentration increases. In fact, at low concentrations of substrate, the electrocatalytic oxidation process is mainly controlled by a diffusion process. In this case, the molecules of alcohol diffuse easily in the bulk of the modified electrode.

However, at higher concentrations, a significant increasing of peak current ( $i_{pa}$ ) due to the interaction between alcohol molecules and available catalytic sites of the modified electrode expresses an enhancement in the electrocatalytic activity. In this case, it was observed that the current density obtained for the oxidation of isopropanol was found to be higher than those of all other alcohols [25]. This result may be explained by a significant increasing of the electronic density on the hydroxylated carbon owing to electrodonating effect of both methyl groups.

The reduction of carbon dioxide ( $\text{CO}_2$ ) has also been investigated. Cyclic voltammograms obtained with GC-electrode modified by electrodeposition of poly-[Cu(II)-L] in acetonitrile solutions are shown in Fig.7. The redox system Cu(II)/Cu(I) appears at -1.100 V/SCE under dinitrogen atmosphere whereas under  $\text{CO}_2$  atmosphere, severe changes are observed such as, a significant enhancement of  $i_{pc}$  current accompanied with total disappearance of  $i_{pa}$  and the shifting of the reduction wave potential inducing 160 mV as gain of potential. This gain of potential is characteristic of an electrocatalytic current represented by the ratio  $i_{pc}(\text{CO}_2)/i_{pc}(\text{N}_2)$  equal to 3.28. Hence, the importance of this ratio permits to judge the efficiency of an electrocatalytic reaction. Furthermore, a new redox system has also appeared at more cathodic potentials ( $E_{1/2} = -1.121\text{V}$ ). This result corroborates with the formation of  $\mu$ -oxo dimers like those described for the oxidation reactions model of cytochrome P450 [26]. The reduction process of carbon dioxide allows to regenerate the catalyst and produces simultaneously carbon monoxide with formic acid as reported in the literature [27]. These facts can be summarized in the following proposed mechanism, illustrated by the Fig.8.

### Figure 8

The main results obtained from this study can be summarized as follow: (i) proposition of a simple and efficient method for the synthesis of new pyrrolic monomers containing transition metals coordinated to the Schiff base ligands. This new class of compounds was



clearly evidenced by cyclic voltammetry and mass spectrometry analysis. (ii) The copper(II)-complex obtained was easily electropolymerized by cathodic reduction process to its poly-[Cu(II)-L] yielding modified electrodes containing catalytic sites as divalent copper ions ( $\text{Cu}^{\text{II}}$ ). (iii) These new modified electrodes can be used as sensors for the detection of small molecules such as carbon dioxide, dioxygen, nitrites and nitrates ions. Finally, it can again be concluded that this electrode material seems to be more adapted for working in catalysis, electrocatalysis and sensors.

### **Acknowledgements:**

The authors wish to thank the Algerian Ministère de l'Enseignement Supérieur et de la Recherche Scientifique for financial support and would like also to thank Professors Anny JUTAND and Christian AMATORE, Ecole Normale Supérieure Département de Chimie, UMR CNRS-ENS-UPMC 8640, 24 rue Lhomond, 75231 Paris Cedex 5. France for their help in spectroscopic characterizations.

### **References**

- [1] M. Aslantas, E. Kendi, N. Demir, A. E. Sabik, M. Tumer, M. Kertmen, Synthesis, spectroscopic, structural characterization, electrochemical and antimicrobial activity studies of the Schiff base ligand and its transition metal complexes, *Spectrochimica Acta Part A*. 74 (2009) 617–624
- [2] A. Bilici, I. Kaya, M. Saçak, Oxidative Polymerization of  $\text{N}_2\text{O}_2$  Type Schiff Base Monomer and Its Metal Complexes: Synthesis and Thermal, Optical and electrochemical Properties, *J Inorg Organomet Polym.* 20 (2010)124–133
- [3] A. Adhikari, S. Radhakrishnan, R. Patil, Influence of dopant ions on properties of conducting polypyrrole and its electrocatalytic activity towards methanol oxidation, *Synth. Met.* 159 (2009) 1682-1688.

- [4] M. Rizzi, M. Trueba, S.P. Trasatti, Polypyrrole films on Al alloys: The role of structural changes on protection performance, *Synth. Met.* 161 (2011) 23-31.
- [5] D.D. Ateh, A. Waterworth, D. Walker, B.H. Brown, H. Navsaria, P. Vadgama, Impedimetric sensing of cells on polypyrrole-based conducting polymers, *J. Biomed. Mater. Res. Part A.* 83A (2007) 391-400.
- [6] I. Kuźniarska-Biernacka, C. Pereira, A. P. Carvalho, J. Pires, C. Freire, Epoxidation of olefins catalyzed by manganese(III) salen complexes grafted to porous heterostructured clays, *Applied Clay Science.* 53 (2011) 195-203.
- [7] J. N. Pedeutour, K. Radhakrishnan, H. Cramail, A. Deffieux, Single-site Olefin Polymerization Catalysts Via the Molecular Design of Porous Silica, *Macromol. Rapid Commun.* 22 (2001) 1095-1123.
- [8] P. Manisankar, A. Gomathi, D. Velayutham, Oxygen reduction at the surface of glassy carbon electrodes modified with anthraquinone derivatives and dyes, *J Solid State Electrochem.* 9 (2005) 601–608.
- [9] A. Rios-Escudero, M. Villagran, F. Caruso, J.P. Muena, E. Spodine, D. Venegas-Yazigi, L. Massa, L.J. Todaro, J.H. Zagal, G.I. Cardenas-Jiron, M. Paez, J. Costamagna, Electrocatalytic reduction of carbon dioxide induced by bis(*N*-*R*-2-hydroxy-1-naphthaldiminato)-copper(II) (*R* = *n*-octyl, *n*-dodecyl): Magnetic and theoretical studies and the X-ray structure of bis(*N*-*n*-octyl-2-hydroxy-1-naphthaldiminato)-copper(II), *Inorganica Chimica Acta.* 359 (2006) 3947–3953.
- [10] (a) A. Ourari, L. Baameur, G. Bouet and A. M. Khan, Is the electrocatalytic epoxidation of stilbene isomers using manganese (III) tetradentate Schiff bases complexes stereoselective?, *Electrochem. Commun.* 10 (2008) 1736-1739, (b) Y. Zidane, A. Ourari, T. Bataille, P. Happiot, D. Hauchard, Electrochemical study with cavity microelectrode

containing clay-supported Mn<sup>(III)</sup>salen complex – Dioxygen activation with cytochrome P450 model, *J. Electroanal. Chem.* 641 (2010) 64-70.

[11] R.J.P. Williams, Metal ions in biological catalysts, *Pure & Appl.Chem.* 54 (1982) 1889-1904.

[12] M. Vilas-Boas, C. Freire, B. de Castro, A. R. Hillman, Electrochemical Characterization of a Novel Salen-Type Modified Electrode, *J. Phys. Chem.* 102 (1998) 8533-8540.

[13] N. Raman, A. Kulandaisamy, C. Thangaraja, P. Manisankar, S. Viswanathan, C. Vedhi, Synthesis, structural characterization and electrochemical and antibacterial studies of Schiff base copper complexes, *Transition Metal Chemistry.* 29 (2004) 129–135.

[14] In a 50-ml three necked flask, equipped with a reflux condenser and magnetic stirrer, 518 mg (2 mmol) of 6-(3'-N-pyrrolpropoxy)-2-hydroxyacetophenone and 60 mg (1 mmol) of ethylenediamine were dissolved in 15 ml of absolute ethanol. This mixture was refluxed for about 1 hour until completion of the reaction. To this solution, 199 mg (1 mmol) of copper acetate monohydrated (Cu (OAc)<sub>2</sub>·H<sub>2</sub>O) dissolved in 10 ml of absolute ethanol were immediately added in one portion. The mixture was heated to reflux under nitrogen atmosphere and stirring again for two other hours and then left overnight in the refrigerator. The complex was precipitated by diethyl oxide and the solid was recovered by filtration, yielding 85 mg (61.2 %): **UV-vis** ( $\lambda_n$  max/nm [- $\epsilon$  (M.cm<sup>-1</sup>)]:  $\lambda_1$  =288 nm [188130],  $\lambda_2$  =351 nm [68040],  $\lambda_3$  =550nm [4560] **.FTIR:**  $\nu_{x-y}$ (cm<sup>-1</sup>):  $\nu_{C-H}$  = 2905;  $\nu_{C=N}$  = 1602;  $\nu_{C-O-C}$  = 1096;  $\nu_{C-H(arom.)}$  = 740;  $\nu_{M-N(arom.)}$  = 625;  $\nu_{M-O(arom.)}$  = 570. **Microanalysis** C<sub>32</sub>H<sub>36</sub>O<sub>4</sub>N<sub>4</sub>Cu (Calc. (found)): **C:** 63.62 (63.54); **H:** 5.96 (6.36); **N:** 9.27 (9.70).

[15] A. Ourari, D. Aggoun, S. Bouacida, 1-{2-Hydroxy-6-[3-(pyrrol-1-yl)propoxy]phenyl} ethanone, *Acta Cryst.* E68 (2012)1083

- [16] E. Franco, E. Lopez-Torres, M. A. Mendiola, M. T. Sevilla, Synthesis, spectroscopic and cyclic voltammetry studies of copper(II) complexes with open chain, cyclic and a new macrocyclic thiosemicarbazones, *Polyhedron*. 19 (2000) 441–451.
- [17] S. Meghdadi, M. Amirnasr, K. Mereiter, H. Molaei, A. Amiri, Synthesis, structure and electrochemistry of Co(III) complexes with an unsymmetrical Schiff base ligand derived from 2-aminobenzylamine and pyrrole-2-carboxaldehyde, *Polyhedron*. 30 (2011) 1651–1656.
- [18] J. Losada, I. D. Peso, L. Beyer, Synthesis, electrochemical properties and electro-oxidative polymerization of copper(II) and nickel(II) complexes with N-benzoylthiourea ligands containing pyrrole groups, *Transition Metal Chemistry*. 25 (2000) 112-117.
- [19] A single crystal was mounted on a Nonius four-circle diffractometer equipped with a CCD camera and a graphite monochromatic Mo K $\alpha$  radiation source ( $\lambda=0.71073 \text{ \AA}$ ) from the Centre de Diffractométrie (CDFIX), de l'Université de Rennes1, France. Intensity data were collected at 293 K and reduced using SCALEPACK program. The structure was solved by direct methods using SHELXS86 program. The refinements were performed by full matrix least squares method based on  $F^2$  values against all reflections and including anisotropic displacement parameters for all non-H atoms using SHELXL97. Drawings of molecules were produced with the program ORTEP-3. All calculations were performed with the WINGX suite of programs.
- [20] F. H. Allen, O. Kennard, D. G. Watson, L. Brammer, A. G. Orpen and R. Taylor, Tables of bond lengths determined by X-ray and neutron diffraction. Part 1. Bond lengths in organic compounds, *J. Chem. Soc. Perkin Trans.* 2(1987) S1–S19.
- [21] P. Talukder, S. Shit, A. Sasmal, S. R. Batten, B. Moubaraki, K. S. Murray, S. Mitra, An antiferromagnetically coupled hexanuclear copper(II) Schiff base complex containing phenoxo and dicyanamido bridges: Structural aspects and magnetic properties, *Polyhedron*. 30 (2011) 1767–1773.

- [22] S. Naskar, S. Naskar, H. Mayer-Figge, W. S. Sheldrick, S. K. Chattopadhyay, Synthesis, X-ray crystal structures, spectroscopic and cyclic voltammetric studies of Cu(II) Schiff base complexes of pyridoxal, Polyhedron. 30 (2011) 529–534.
- [23] A. Deronzier, J. C. Moutet, Polypyrrole films containing metal complexes: syntheses and applications, Coordination Chemistry Reviews. 147 (1996) 339-371.
- [24] S. Sreedaran, K. Shanmuga Bharathi, A. Kalilur Rahiman, L. Jagadish, V. Kaviyaranan, V. Narayanan, Novel unsymmetrical macrocyclic dicompartmental binuclear copper(II) complexes bearing 4- and 6-coordination sites: Electrochemical, magnetic, catalytic and antimicrobial studies, Polyhedron. 27 (2008) 2931–2938.
- [25] K. L. Nagashree, M. F. Ahmed, Electrocatalytic oxidation of methanol on Ni modified polyaniline electrode in alkaline medium, J Solid State Electrochem. 14(2010) 2307–2320
- [26] C.P. Horwitz, S.E. Creager, R.W. Murray, Electrocatalytic olefin epoxidation using manganese Schiff-base complexes and dioxygen, Inorg. Chem. 29 (1990) 1006-1011.
- [27] M. Isaacs, J.C. Canales, M.J. Aguirre, G. Estiu, F. Caruso, G. Ferraudi, J. Costamagna, Electrocatalytic reduction of CO<sub>2</sub> by aza-macrocyclic complexes of Ni(II), Co(II), and Cu(II). Theoretical contribution to probable mechanisms, Inorganica Chimica Acta. 339 (2002) 224-232.

## **List of captions**

### **Tables**

**Table 1.** Crystal data and structure refinement for Cu(II)-L

**Table 2.** Roughness and thickness of poly-[Cu(II)-L]

### **Schemes**

**Scheme 1.** Reaction way leading to the formation of the pyrrolic monomers.

### **Figures**

**Fig.1.** X-ray molecular structure of **Cu(II)-L** with the atomic numbering scheme. Selected bond lengths (Å) and bond angles (°) : Cu—O2 1.892 (3), Cu—O1 1.899 (3), Cu—N1 1.937 (3), Cu—N2 1.947 (3), O2—Cu—O1 92.54 (12), O2—Cu—N1 170.02 (13), O1—Cu—N1 90.67 (12), O2—Cu—N2 92.37 (12), O1—Cu—N2 168.64 (13), N1—Cu—N2 86.22 (13), C12—O1—Cu 124.5 (2), C21—O2—Cu 126.4 (2), C14—N1—Cu 128.8 (3), C16—N1—Cu 110.6 (2), C18—N2—Cu 128.0 (3), C17—N2—Cu 110.2 (2)

**Fig.2.** Packing of the molecules along the *a* direction.

**Fig.3.** Cyclic voltammogram of 1 mM Cu(II)-L at GC electrode in acetonitrile solution, 0.1 M, TBAP. Scan rate 100 mV s<sup>-1</sup>.

**Fig.4.** Cyclic voltammogram showing electrodeposition of poly-[Cu(II)-L] onto a glassy-carbon electrode in acetonitrile 0.1 M in TBAP, scan rate: 100 mVs<sup>-1</sup>.

**Fig.5.** AFM images obtained for the polymerized films from Cu(II)-L at several cyclical scans; (A): 1 cycle; (B): 10 cycles; (C): 30 cycles; (D): 50 cycles; on ITO electrodes.

**Fig.6.** Plots of the anodic oxidation charge ( $Q_{ox}$ ), recorded for various volumes (μl) of each one of the studied alcohols.

**Fig.7.** Voltammograms of the electrocatalytic reduction of CO<sub>2</sub> with poly-Cu(II)-L on GC-electrode under dinitrogen (N<sub>2</sub>) (—, full line) and under (CO<sub>2</sub>) atmosphere (-----, dotted line).

**Fig.8.** Proposed electrocatalytic cycle

**Table 1.**

Molecular formula	C <sub>32</sub> H <sub>36</sub> CuN <sub>4</sub> O <sub>4</sub>
Molecular weight	604.19
Temperature (K)	293
Radiation $\lambda$	Mo-K $\alpha$ (0.71073 Å)
Crystal system	Triclinic
Space group	P-1
$a/\text{Å}$	7.9688 (4)
$b/\text{Å}$	12.8433 (9)
$c/\text{Å}$	14.5166 (11)
$\alpha^\circ$	102.075 (3)
$\beta^\circ$	90.486 (4)
$\gamma^\circ$	96.270 (4)
$V/\text{Å}^3$	1443.40 (17)
Z	2
$D_{\text{calc}}$ (g cm <sup>-3</sup> )	1.39
Crystal size (mm <sup>3</sup> )	0.1 × 0.08 × 0.05
Crystal description	Prism
Crystal colour	Colourless
Absorption coefficient (mm <sup>-1</sup> )	0.08
$F(0\ 0\ 0)$	634
Reflections collected/unique	8130/4945 [ $R_{\text{int}} = 0.035$ ]
Range/indices ( $h, k, l$ )	-9, 9; -15, 15; -17, 17
$\theta_{\text{limit}}$	2.4– 25.3
No. of observed data, $I > 2\sigma(I)$	3660
No. of variables	370
No. of restraints	0
Goodness of fit on $F^2$	0.154
Largest diff. Peak and hole (e Å <sup>-3</sup> )	0.43 and -0.46

$$R = \{\Sigma[w(|F_0| - |F_c|)] / \Sigma w(|F_0|)\}, R_w = \{\Sigma[w(|F_0| - |F_c|)^2] / \Sigma w(|F_0|^2)\}^{1/2},$$

$$wR_2 = \{\Sigma[w(F_0^2 - F_c^2)^2] / \Sigma w(F_0^2)\}^{1/2}$$

$$w = 1/[\sigma^2(F_o^2) + (0.0794P)^2 + 0.6853P] \text{ where } P = (F_o^2 + 2F_c^2)/3$$

**Table 2.**

Number of cyclical scans	1	5	10	20	30	50
Thickness (nm)	166.90	321.38	125.71	246.61	757.19	729.65
Roughness (nm)	1.9180	6.4787	8.1671	21.8772	58.6395	75.1424

**Scheme 1.**

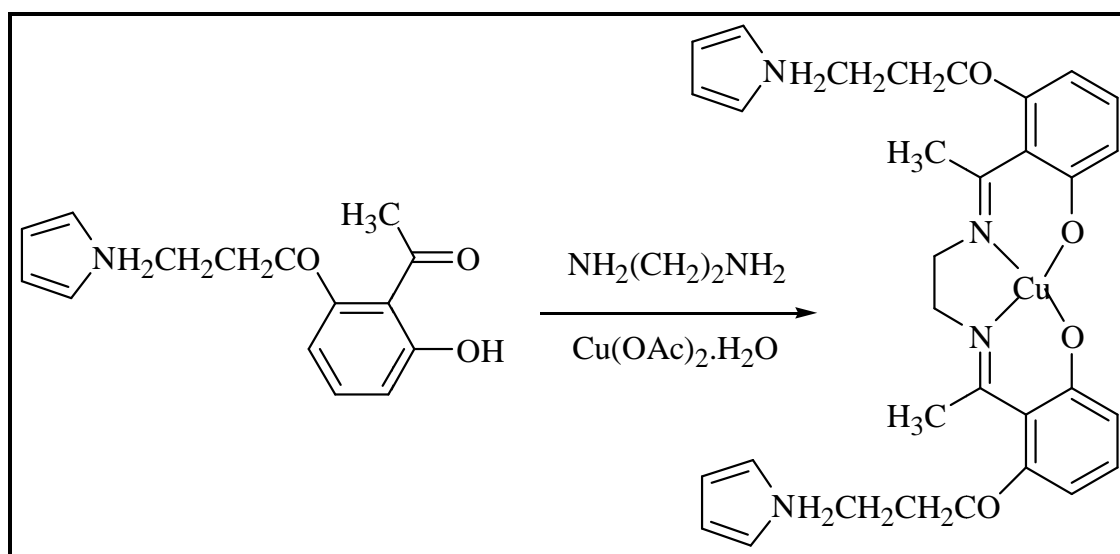


**Fig.1.**

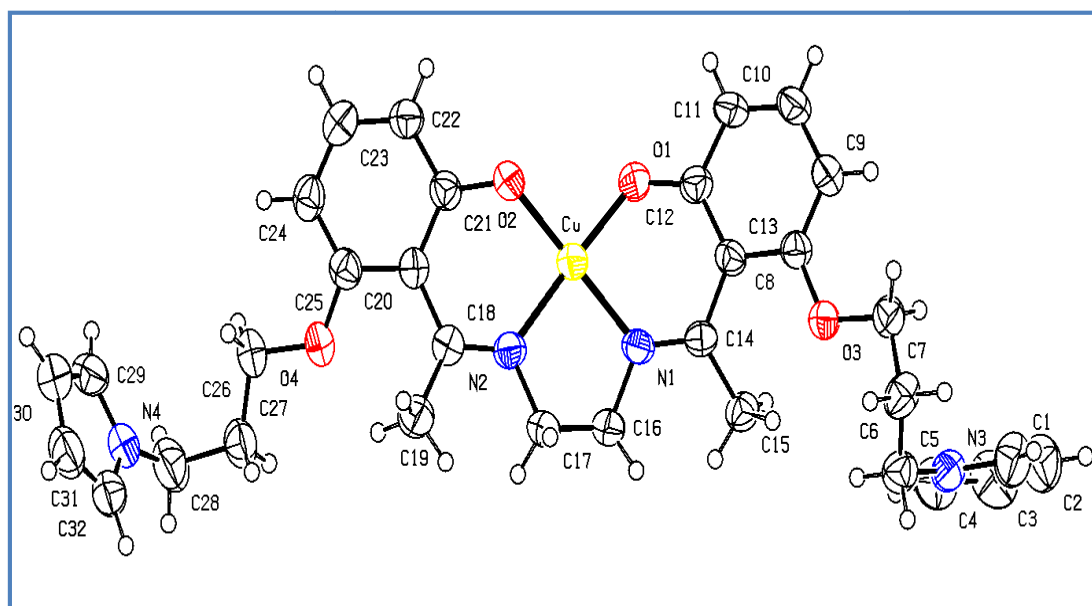




Fig.2.

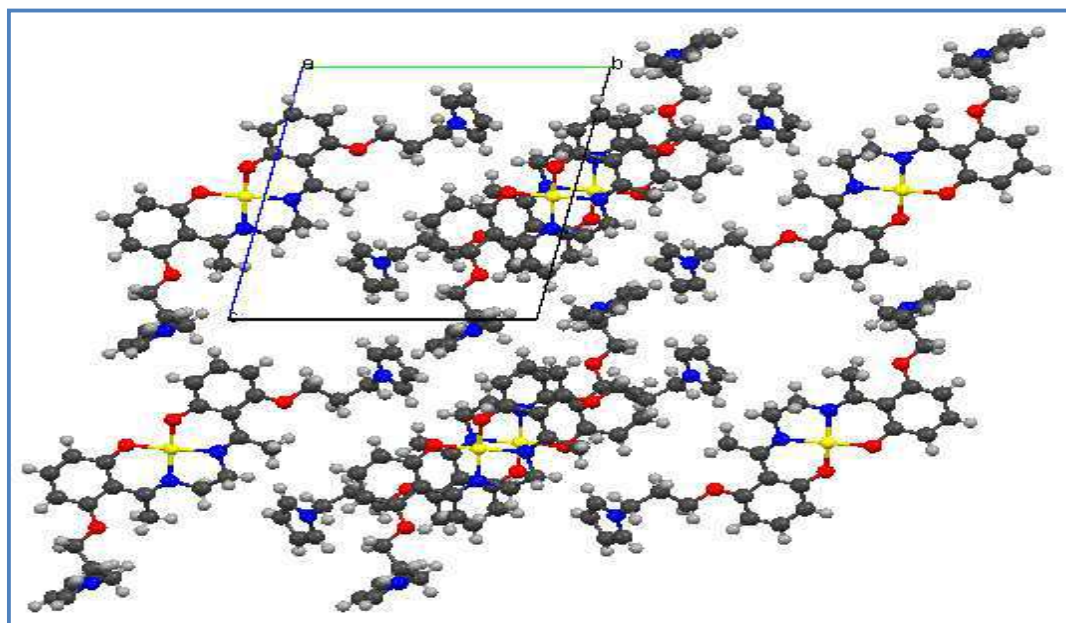


Fig.3.

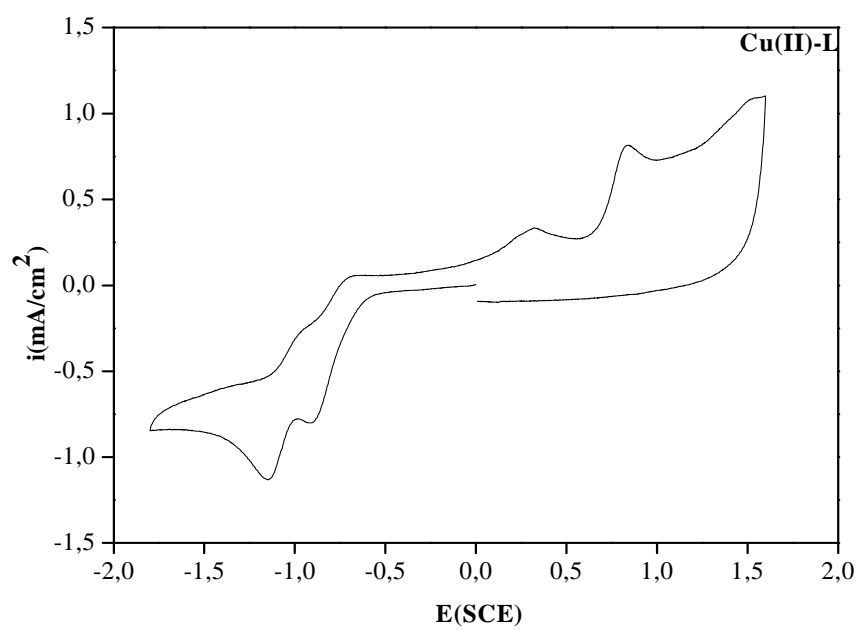
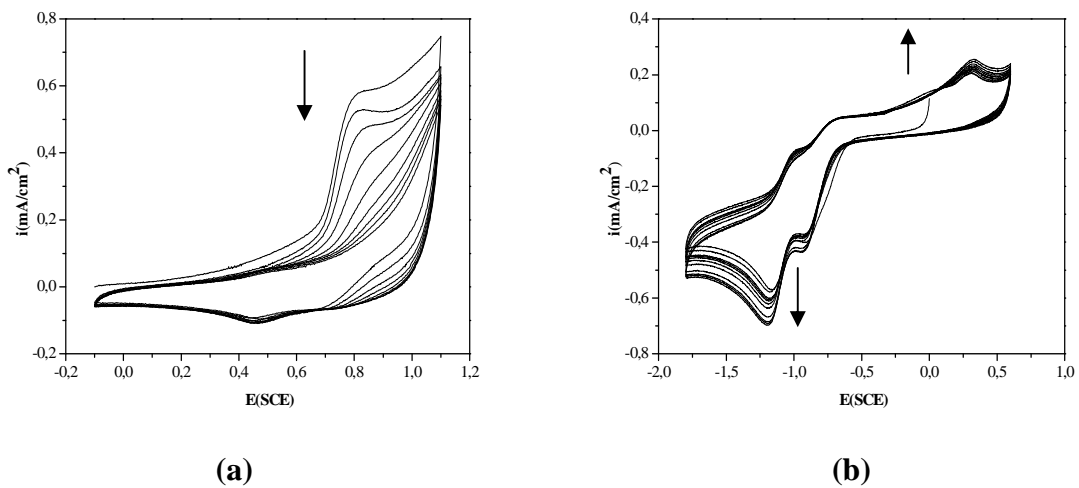
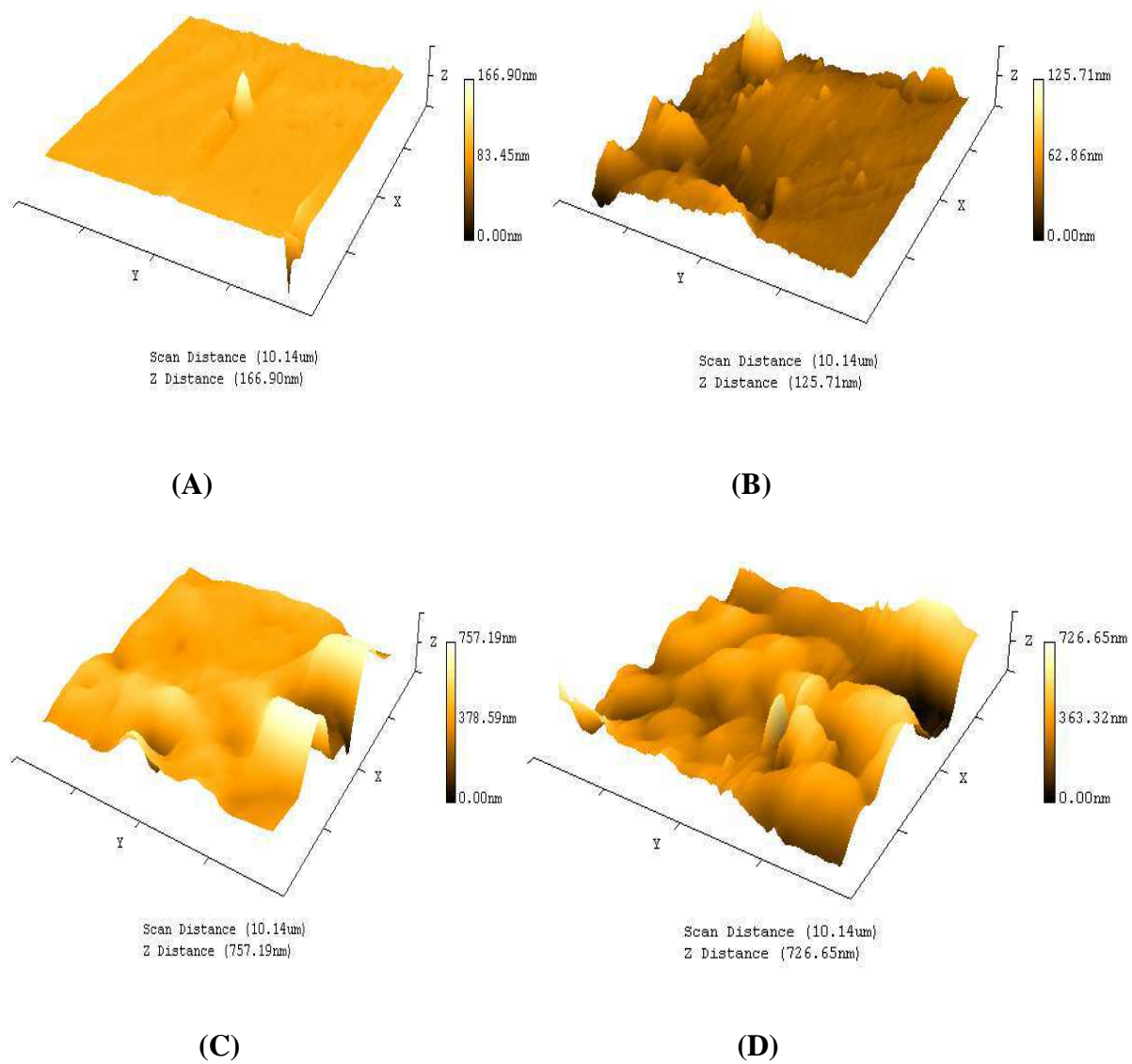


Fig.4.



**Fig.5.**



**Fig.6.**

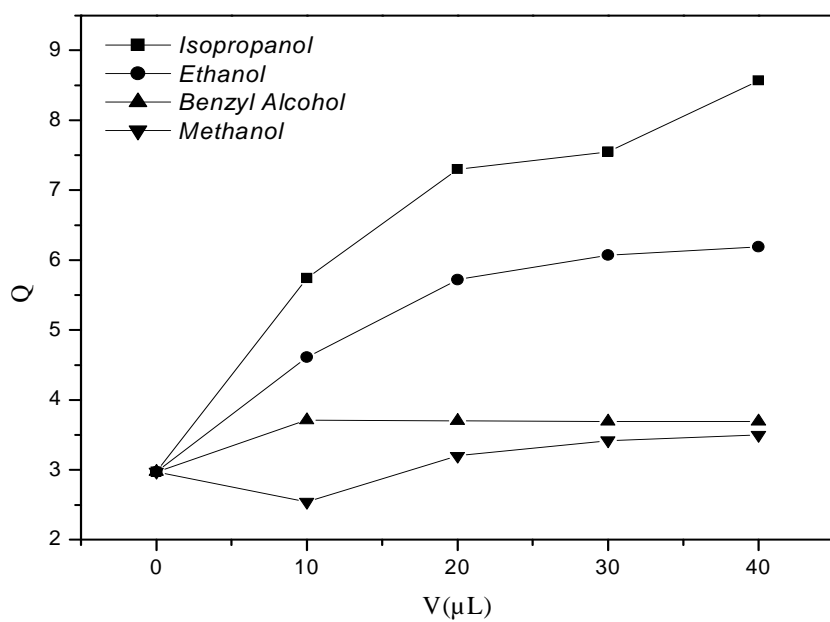


**Fig.7.**

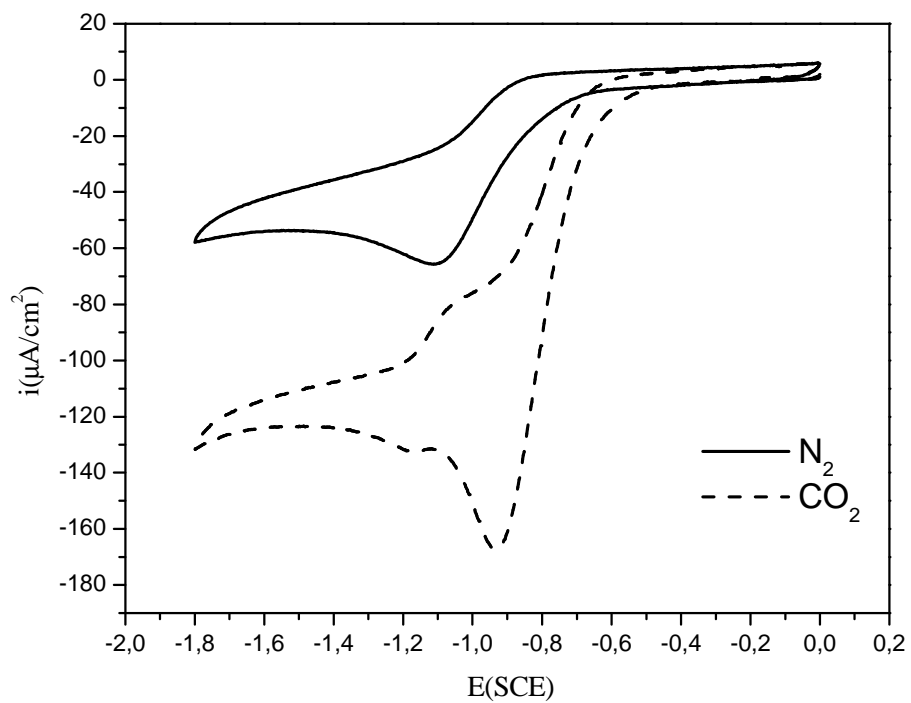


Fig.8.

